University of Groningen

Mitral Valve Coaptation Reserve Index

Jainandunsing, Jayant S.; Massari, Dario; Vos, Jaap Jan; Wijdh-den Hamer, Inez J.; van den Heuvel, Ad FM; Mariani, Massimo A.; Mahmood, Feroze; Bouma, Wobbe; Scheeren, Thomas W.L.

IMPORTANT NOTE: You are advised to consult the publisher's version (publisher's PDF) if you wish to cite from it. Please check the document version below.

Document Version
Version created as part of publication process; publisher's layout; not normally made publicly available

Link to publication in University of Groningen/UMCG research database

Original Article

Mitral Valve Coaptation Reserve Index: A Model to Localize Individual Resistance to Mitral Regurgitation Caused by Annular Dilation

Jayant S. Jainandunsing, MD[*,1], Dario Massari, MD[*],
Jaap Jan Vos, MD, PhD[*], Inez J. Wijdh-den Hamer, MD[†],
Ad FM van den Heuvel, MD, PhD[‡],
Massimo A. Mariani, MD, PhD[†], Feroze Mahmood, MD, PhD[§],
Wobbe Bouma, MD, PhD[†], Thomas W.L. Scheeren, MD, PhD[*]

[*]Department of Anesthesiology, University of Groningen, University Medical Center Groningen, Groningen, the Netherlands
[†]Department of Cardiothoracic Surgery, University of Groningen, University Medical Center Groningen, Groningen, the Netherlands
[‡]Department of Cardiology, University of Groningen, University Medical Center Groningen, Groningen, the Netherlands
[§]Department of Anesthesiology, Beth Israel Deaconess Medical Center, Harvard Medical School, Boston, MA

Objectives: The objective of this study was to develop a mathematical model for mitral annular dilatation simulation and determine its effects on the individualized mitral valve (MV) coaptation reserve index (CRI).

Design: A retrospective analysis of intraoperative transesophageal 3-dimensionalechocardiographic MV datasets was performed. A mathematical model was created to assess the mitral CRI for each leaflet segment (A1-P1, A2-P2, A3-P3). Mitral CRI was defined as the ratio between the coaptation reserve (measured coaptation length along the closure line) and an individualized correction factor. Indexing was chosen to correct for MV sphericity and area of largest valve opening. Mathematical models were created to simulate progressive mitral annular dilatation and to predict the effect on the individual mitral CRI.

Setting: At a single-center academic hospital.

Participants: Twenty-five patients with normally functioning MVs undergoing cardiac surgery.

Interventions: None.

Measurements and Main Results: Direct measurement of leaflet coaptation along the closure line showed the lowest amount of coaptation (reserve) near the commissures (A1-P1 0.21 ± 0.05 cm and A3-P3 0.22 ± 0.06 cm), and the highest amount of coaptation (reserve) at region A2 to P2 0.25 ± 0.06 cm. After indexing, the A2-to-P2 region was the area with the lowest CRI in the majority of patients, and also the area with the least resistance to mitral regurgitation (MR) occurrence after simulation of progressive annular dilation.

Conclusions: Quantification and indexing of mitral coaptation reserve along the closure line are feasible. Indexing and mathematical simulation of progressive annular dilatation consistently showed that indexed coaptation reserve was lowest in the A2-to-P2 region. These results may explain why this area is prone to lose coaptation and is often affected in MR.
© 2022 The Authors. Published by Elsevier Inc. This is an open access article under the CC BY license (http://creativecommons.org/licenses/by/4.0/)

Key Words: echocardiography; mitral valve; coaptation; mitral regurgitation; mitral valve coaptation reserve index

[1]*Address correspondence to* Jayant Shyam Jainandunsing, MD, University Medical Centre Groningen, Hanzeplein 1, the Netherlands, Groningen 9700 RB.

E-mail address: jsjainandunsing@gmail.com (J.S. Jainandunsing).

The mitral valve (MV) apparatus is a dynamic cardiac structure that aims to maintain left ventricular systolic competence and diastolic nonrestriction. The coaptation zone of the valve

is critical to valve competency and to preserving valve integrity. It is defined as the area of apposition between the anterior and posterior leaflets during left ventricular systole. This coaptation zone is the area that endures the highest levels of mechanical stress during valve closure, where opposing forces from both leaflets interact.[1]

Identification and quantification of the amount of coaptation (reserve), the contact area between the anterior and posterior leaflet, may play an important role in determining an MV's ability to sustain geometric distortions and its resistance to develop mitral regurgitation (MR).[2,3]

In this study, the authors created a model to quantify the MV coaptation zone along the MV leaflet closure line, with correction for an individualized factor by indexing (the MV coaptation reserve index [MV CRI]). They hypothesized that their model could predict the location of MR and that the regions of the lowest coaptation reserve would not consistently correspond to a low CRI.

In addition, the study authors sought to develop a mathematical simulation model for annular dilatation and to determine its geometric effects on the individualized MV CRI.

Methods

This study was designed as a single-center retrospective feasibility study of prospectively collected data. Data analysis was performed as part of an Institutional Review Board-approved protocol of intraoperative data collection, with a waiver of informed consent.

Patients and Image Acquisition

Intraoperative real-time 3-dimensional transesophageal echocardiography (RT-3D TEE) and subsequent MV analysis were performed in 25 patients, with normally functioning MVs (<mild), undergoing cardiac surgery for indications other than MV disease between July 2016 and April 2018 (Table 1). Intraoperative RT-3D TEE was performed as part of routine intraoperative care, as described in the authors' institution's perioperative imaging protocol for all patients undergoing cardiac surgery. The 3D echocardiographic datasets were acquired after the induction of general anesthesia and before sternotomy, using a Vivid E9 ultrasound system and a GE 6VT-D, 4D TEE transducer (General Electric, Healthcare, Hoevelaken, NL). A standard midesophageal 4-chamber view, with a frame rate of 15-to-25 Hz, focus on the MV, and full inclusion of the MV was used to obtain the 3D echocardiographic datasets.

The selection of data was narrowed to those patients in whom complete 3D echocardiographic datasets of the MV were available for off-line postprocessing and analysis, with no stitching artifacts (exclusion criterion). All 3D echocardiographic datasets were collected by the same anesthesiologist.

Image Segmentation and Annular and Leaflet Modeling

Each full-volume 3D TEE data set was exported from Echo-Pac version 201 (General Electric, Healthcare, Hoevelaken,

Table 1
Demographics

Male/Female sex, n	21/4
Age, y	64.6 ± 8.8
Weight, kg	87 (83-94)
Height, cm	175.9 ± 9.3
Body surface area, m^2	2.05 ± 0.23
Body mass index, kg/m^2	28.6 ± 4.0
Type of surgery, n	20 CABG
	2 AVR
	1 Bentall
	1 Lansac
	1 other
Mitral insufficiency, n	10 none
	15 trace
EuroSCORE II	1.6 (1.1-1.9)
Comorbidities, n	10 arterial hypertension
	3 COPD
	6 diabetes
	5 cerebrovascular disease

Abbreviations: AVR, aortic valve replacement; CABG: coronary artery bypass graft; COPD, chronic obstructive pulmonary disease; EuroSCORE, European System for Cardiac Operative Risk Evaluation.

NL) to a separate computer workstation with TomTec Image Arena software and the semiautomated 4D MV assessment package (TomTec Imaging Systems GmbH, Munich, Germany). All analyses were performed at midsystole. The MV parameters included in the analysis were MV anterior-posterior (AP) diameter, MV anterolateral-posteromedial (AL-PM) diameter, sphericity index of the MV saddle shape, nonplanarity angle, annular circumference, annular area, annular height, and commissural diameter.[4]

Mitral Coaptation Analysis

The MV closure line was identified by the semiautomated 4D MV assessment package. To assess mitral coaptation, the authors identified 7 coaptation points along the mitral closure line by placing 5 vertical lines through the MV closure line (Figs. 1 and 2). The coaptation points were set individually by rotating the multiplanar reformatting lines (yellow, blue, and purple; Fig 1) while maintaining equal distances between the lines, starting with the first point right in the middle (A2-P2). The following 7 coaptation points were identified: the anterior commissure (k1), A1-P1 (k2), midpoint between A1-P1 and A2-P2 (k3), A2-P2 (k4), midpoint between A2-P2 and A3-P3 (k5), A3-P3 (k6), and the posterior commissure (k7). Finally, MV coaptation length at each of the 7 coaptation points was traced manually in the corresponding 2D image (Fig 1).

Annular Dilatation Modeling and CRI

To determine the effect of progressive annular dilatation on the location of loss of coaptation along the closure line, the authors created a 2D model of the MV (Fig 2) for simulation purposes. The model was customized for each patient, with the following individual parameters: AP diameter and AL-PM diameter, closure line length, and A2-P2 coaptation length.
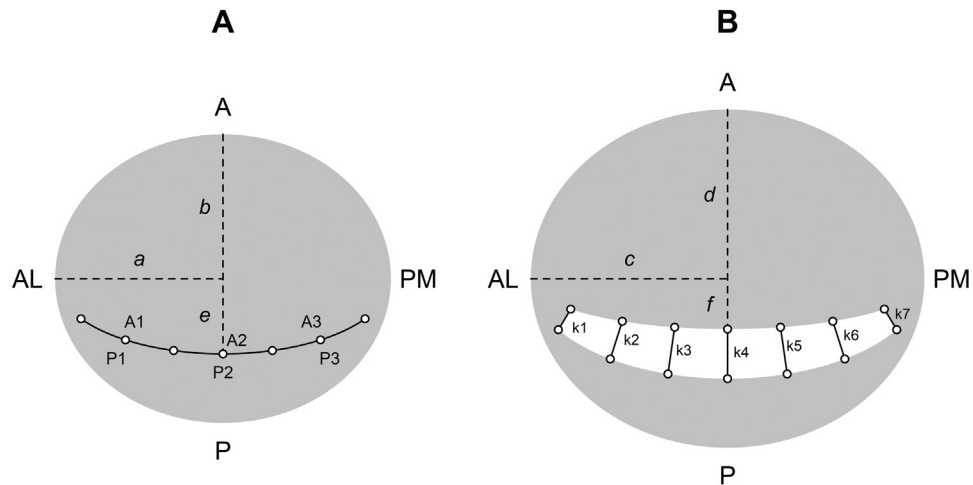
Fig 1. Mitral valve analysis was performed using TomTec Image Arena software. The closure line is divided into 6 equal segments by 7 coaptation points. The coaptation length (coaptation reserve) was manually traced for each point. A, Anterior; P, Posterior; AL, Anterolateral; PM, Posteromedial; A1, A2, A3, anterior mitral valve leaflet segments; P1,P2,P3, posterior mitral valve leaflet segments; K1-K6, six coaptation segments of the contact area; a,b,c,d,e,f , see equation 1 to 4 in the main text.
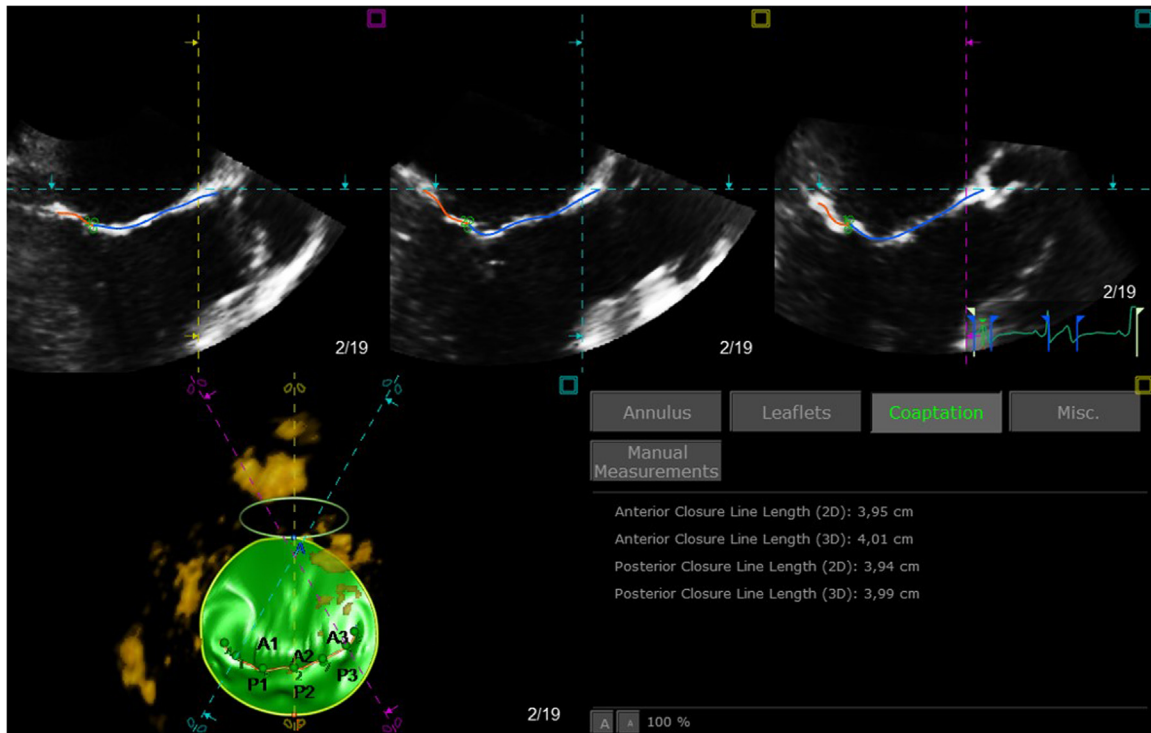

Fig 2. Individualized mitral valve model, (A) before and (B) after simulated mitral annulus dilation.

In the model, the mitral annulus is described by the equation of an ellipse (Equation 1), where a is the major semiaxis (half of the AL-PM diameter), and b is the minor semiaxis (half of the AP diameter).

$$a = \frac{AL - PM \; diameter}{2}$$
$$b = \frac{AP \; diameter}{2} \qquad (1)$$
$$y = \frac{b}{a}\sqrt{a^2 - x^2}$$

The closure line is described by the equation of a semiellipse (Equation 2), where e is the minor semiaxis and is calculated to obtain a closure line length matching the one that was measured in each patient (Equation 3). In the model, the closure line starts and ends slightly inside the ellipse perimeter representing the annulus (Fig 2), and this is obtained by introducing the arbitrary constant 1.33 in Equation 3. The constant was introduced to make the closure line start inside the perimeter of the ellipse. This was necessary to avoid a mathematical artifact; if the commissure points (k1-k7) were drawn on the

perimeter of the ellipse, the model would not be able to simulate the displacement of these points that would remain in the same position.

$$y_2 = \frac{e}{a}\sqrt{a^2 - x^2} \qquad (2)$$

$$e = \sqrt{2 \cdot \left(\frac{1.33 \cdot closure\ line\ length}{\pi}\right)^2 - a^2} \qquad (3)$$

Again, 7 coaptation points were defined at equal distances along the closure line, corresponding to the 7 coaptation points measured in the authors' cohort. Afterward, a symmetrical dilatation of the mitral annulus was simulated by increasing the dimensions of the ellipse. First, for each patient, the authors calculated the hypothetical increase (k) in the AP diameter necessary to lose coaptation at A2-P2. As an example, an increase $k = 1.1$ corresponds to a 10% increase in the AP diameter.

$$k = 1 + \frac{A2 - P2\ coaptation\ length\ \cdot 2}{AP\ diameter}$$

The semiaxes of the enlarged ellipse were calculated as follows and were used to draw the new ellipse (Equation 4; Fig 2, B).

$$c = k \cdot a$$
$$d = k \cdot b \qquad (4)$$
$$y_3 = \frac{d}{c}\sqrt{c^2 - x^2}$$

To simulate the displacement of the commissure points, the linear distances among the commissure line and the anterior and posterior annulus, respectively, were computed along the y axis in the first ellipse, and were kept constant when increasing the dimensions of the ellipse (eg, b + e = d + f in Fig 2). Finally, 7 points were drawn at equal distances along the free border of both mitral leaflets, and the linear distance between each couple of points was computed (*k1* to *k7*; Fig 2 A and B). By dividing each of these values by *k4* (the largest distance corresponding to the A2-P2 coaptation point), the authors obtained the relative proportions of each segment. They defined these values as correction factors (*j1* to *j7*). By using the measured AP and AL-PM diameters, closure line length, and A2-P2 coaptation length for each patient, the correction factors were individualized (Table 1). The coaptation length was indexed against the anatomic characteristics of the MV that are included in the mathematical model (ie, the anterior-posterior and anterolateral-posteromedial diameters, the closure line length and the A2-P2 coaptation length).

The study authors defined the CRI as the ratio between the coaptation reserve (measured coaptation length) and the respective (individualized) correction factor. Indexing was chosen to correct for MV sphericity and area of the largest valve opening.[4,5] Therefore, the CRI should be considered as an estimation of the coaptation reserve that considers both the measured coaptation length and the position of the coaptation points along the closure line. The individualized application of

the model to each patient is shown in the Supplemental material (Supplementary Fig S1). The total time from image acquisition to data analysis was, on average, 15 minutes per patient.

Statistics

The continuous variables are expressed as mean ± SD or median (IQR) depending on data distribution. The categoric variables are expressed as percentages. The normal distribution of continuous data was tested with the Shapiro-Wilk test. The coaptation reserve and the CRI were compared among different coaptation points with a repeated-measures analysis of variance after checking normality and sphericity assumptions. Afterward, pairwise comparisons were performed with the Student's *t* test and corrected for multiple comparisons according to Bonferroni. To avoid an excessive increase in the chance of a type II error, only the A2-P2 coaptation point was compared to the others 6 coaptation points (6 multiple comparisons). The mitral annular area was indexed to the body surface area according to the Du Bois formula. All tests were performed 2-tailed, and a p value < 0.05 was considered statistically significant. R software (version 4.0) was used for statistical analysis (R Foundation for Statistical Computing, Vienna, Austria).

Results

Baseline Characteristics

The median age was 68 years (range 49-79); 4 patients were women, and 21 were men. Twenty patients underwent coronary artery bypass grafting, 2 patients underwent aortic valve replacement, 1 had a Bentall procedure, 1 a Lansac procedure, and 1 patient had urothelial carcinoma with tumor growth into the vena cava. The MR was scored 0 (absent) in 10 patients and trace in 15 patients.

Annular Geometry

The annular geometric values were all in the normal range, as shown in Table 2 and 3.

Coaptation and CRI

The coaptation reserve and the CRI at each coaptation point along the closure line were charted for each patient (Fig 3). When looking at the raw data (gray area in Fig 3), the mean coaptation reserve was lower at the A1-P1 commissure compared to the A2-P2 region. In contrast, after indexing using an individualized correction factor (green area in Fig 3), the average CRI was significantly higher at both commissures and at A1-P1 and A3-P3 as compared to A2-P2 (Table 1).

Similarly, from the raw data (direct measurements of coaptation), it appeared that the point with the lowest coaptation reserve was located at the commissures in 60% of patients, although it was never located at the A2-P2 region (Fig 4, A). After indexing the values, however, the point with the lowest

Table 2
Correction Factors and Coaptation Reserve (Index)

Coaptation Point		Correction Factor				Coaptation Reserve, cm	Coaptation Reserve Index, cm
		Mean	Median	Min	Max		
A2-P2	j4	1				0.25 ± 0.06	
A1/A2-P1/P2	j3	0.948	0.951	0.926	0.963	0.25 ± 0.06	0.26 ± 0.07
A2/A3-P2/P3	j5					0.26 ± 0.06	0.27 ± 0.07
A1-P1	j2	0.780	0.790	0.699	0.843	0.27 ± 0.06	0.34 ± 0.07*
A3-P3	j6					0.26 ± 0.07	0.34 ± 0.09*
A1-P1 commissure	j1	0.458	0.466	0.323	0.594	0.21 ± 0.05*	0.46 ± 0.13*
A3-P3 commissure	j7					0.23 ± 0.06	0.52 ± 0.14*

NOTE. Summary of the individualized correction factors, coaptation reserve and coaptation reserve index.

  * $p < 0.001$ versus A2-P2 (the statistical significance for multiple comparisons was set at $p < 0.008$).

Table 3
Mitral Valve Data

	Mean ± SD	Median	Min	Max
AP-diameter, cm	3.28 ± 0.41	3.25	2.20	4.20
AL-PM diameter, cm	3.57 ± 0.41	3.59	2.75	4.61
Commissural diameter, cm	3.52 ± 0.40	3.52	2.73	4.53
Sphericity index	0.92 ± 0.06	0.93	0.80	1.01
Closure line length, cm	3.31 ± 0.40	3.34	2.50	4.15
Annular circumference, cm	11.5 ± 1.3	11.5	8.3	14.8
Annular area, cm^2	9.4 ± 2.2	9.3	4.9	15.4
Annular area, cm^2/m^2	4.6 ± 1.0	4.5	2.9	7.7
Annular height, cm	0.85 ± 0.16	0.84	0.49	1.12
Non-planarity angle, degrees	141.5 ± 9.4	140.1	125.0	161.3

Abbreviations: AL-PM, anterolateral-posteromedial; AP, anterior-posterior.

CRI turned out to be A2-P2 or a nearby segment in 44% and 48% of patients, respectively (Fig 4, B). In only 2 patients, the A1-P1 or A3-P3 points corresponded to the lowest CRI. Summarizing the data, in fewer than one-third (28%) of the patients, the point of lowest CRI corresponded to the point of

Fig 3. Coaptation reserve (*gray*) and coaptation reserve index (*green*). *$p < 0.001$ versus A2-P2.

lowest measured coaptation reserve. The data for each patient are presented in the Supplemental material (Supplementary Fig S2).

Annular Dilatation Modeling and CRI

Because the point with the lowest CRI is expected to be the first to lose coaptation when the mitral annulus dilates, based on the definition given previously, the authors used the model to simulate in each patient various fixed percentage increases of the mitral annular area. Three representative examples are shown in Fig 5, which presents the expected reduction of the coaptation reserve after a simulated 10%, 30%, and 50% increase in the mitral annular area. In the hypothetical average patient, the first point to lose coaptation will be A2-P2 (Fig 5, A). In patient 14 (Fig 5, B), the lowest coaptation reserve was located at the commissures, but A2-P2 is expected to lose coaptation first, having the lowest CRI. Alternatively, in patient 22 (Fig 5, C), A3-P3 was the first point to lose coaptation, having the lowest coaptation reserve even after indexing the value. The simulations for the other patients are shown in the Supplemental material (Supplementary Fig S3).

Echocardiographic Location of MR and CRI

Fifteen patients had mild-to-trace MR, preoperative transthoracic echocardiogram data were analyzed, and the location of MR was scored blindly. In 10 out of 15 patients, the MR location matched with the calculated lowest CRI, and in 5 patients, the lowest calculated CRI was in the region between A1-P1 and A2-P2 but was scored at the A1-P1 region on echocardiography images.

Discussion

In this study, the authors calculated an individualized MV CRI to assess the areas of least coaptation between the anterior and posterior MV; they also constructed a mathematical simulation model for annular dilatation.

Most studies analyzing MV coaptation were performed in surgical patients after MV plasty.[5,6] Only 1 study did a quantitative assessment of the MV coaptation zone and defined a
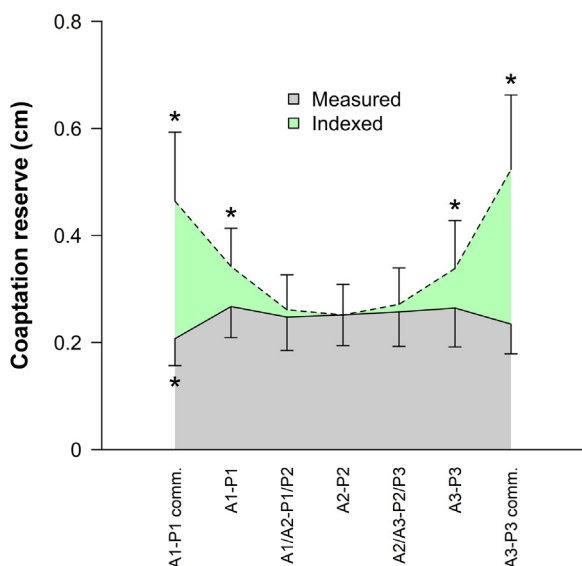
6   *J.S. Jainandunsing et al. / Journal of Cardiothoracic and Vascular Anesthesia 00 (2022) 1−8*
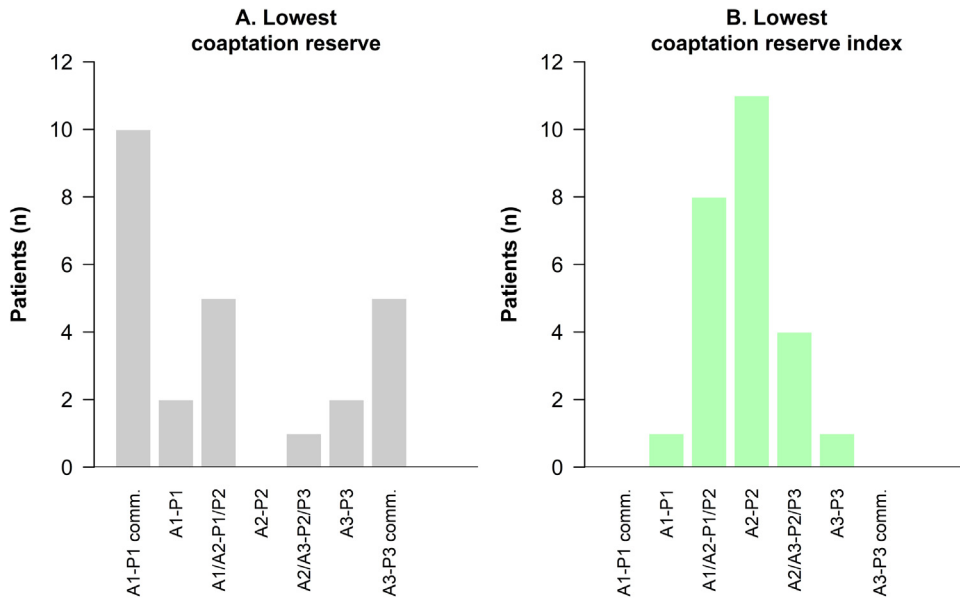

Fig 4. (A) Point of lowest coaptation reserve and (B) lowest coaptation reserve index.

coaptation index in functional MR patients, and the authors demonstrated with analysis of variance that the coaptation index was associated with the severity of functional MR and that there also was a correlation between the 2D vena contracta and the coaptation index.[2] In the authors' study, they used an index based on the following parameters: AP diameter; AL-PM diameter; closure line length; and the A2-P2 coaptation length, derived from 3D datasets. The authors' population was different in the way that they had either no or trace MR. With regard to the 15 patients with mild MR, 10 patients had MR scored on transthoracic echocardiogram comparable with the region with the lowest CRI. Five patients had MR scored at A1-P1, whereas the lowest CRI was between A1/P1-A2/P2. Reasons for this discrepancy could be that the authors' measured coaptation area was done on more accurate 3D data or

the tendency to choose for a certain location (segment 1, 2, or 3) rather than guessing an in-between location. Although 2D-echocardiography is operator-dependent and requires the finesse of probe manipulation to delineate MV pathology compared to 3D, the authors had similar results in two-thirds of their patients; and in the remaining one-third of patients, they had a slight difference in location. For future analysis, the best option is to compare trace MR from 3D-color Doppler datasets, from which the location of the MR can be mor accurately assessed, with the lowest CRI; unfortunately, in the authors' patient population, they did not have 3D-color Doppler data available.

The strengths of the authors' model compared to more complex 3D analysis previously published were the following: (1) it can be performed within 15 minutes compared to 3 hours,[2]
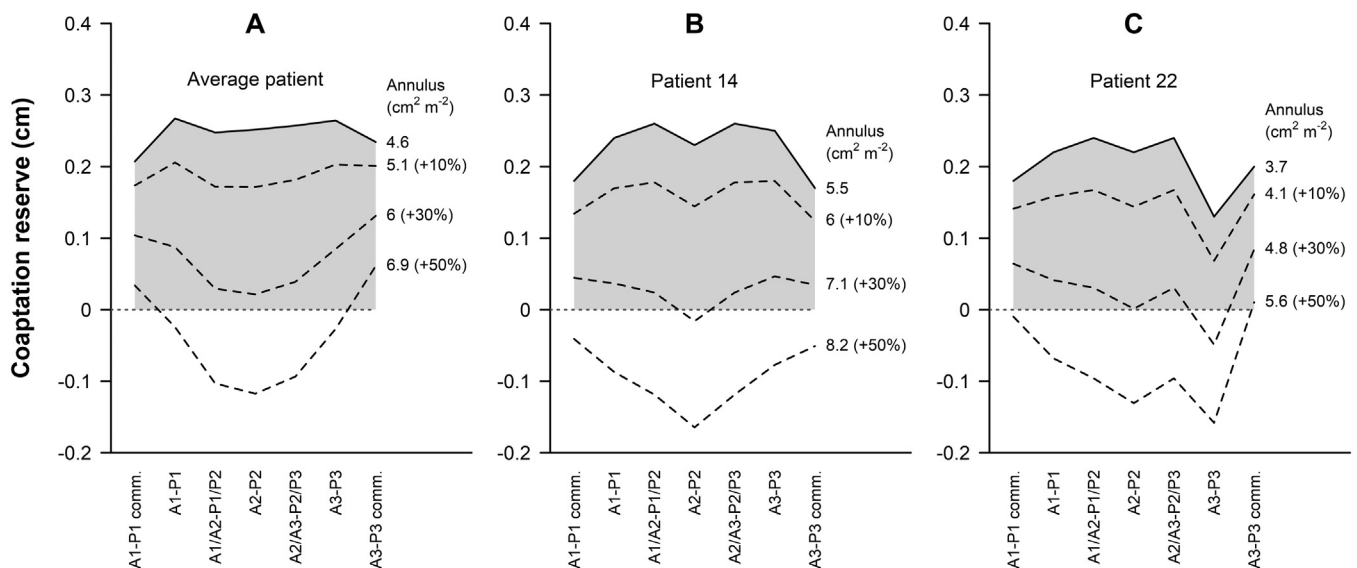

Fig 5. Simulation of progressive mitral annulus area increases in (A-C) 3 typical patients. The *solid line* represents the measured coaptation reserve. The *dashed lines* represent the simulated coaptation reserve after increasing the mitral annulus area.

(2) 2D datasets can be used if accurately obtained instead of 3D acquired MV area, and (3) the authors were able to construct a mathematical model mimicking MV annular dilation.

Direct measurement of leaflet coaptation along the closure line showed the lowest amount of coaptation (reserve) near the commissures in most patients of the authors' cohort. In only a few patients, the A2-P2 area showed the lowest amount of coaptation. This may be explained by the hypothesis that the coaptation reserve is not only related to the absolute value of the measured coaptation length, but also to the position of the coaptation point along the closure line. In addition, the coaptation area tapers toward the sides when it reaches the commissures, which explains the relatively smaller coaptation lengths toward the commissures (this study). Literature has shown when the mitral annulus dilates, the central coaptation points are likely to be displaced to a greater extent than the points that are closer to the commissures.[7-10] In order to account for this, the study authors indexed the coaptation length at 7 points along the MV closure line for each patient to calculate the MV CRI. After indexing, the A2-P2 region was the area with the lowest CRI in the majority of patients, and it also was the area with the least resistance to MR after simulation of progressive annular dilation. These findings are physiologically plausible in that they demonstrated that the commissural regions are most likely to exhaust coaptation reserve with leaflet tethering, and the central region is geometrically suited to sustain annular dilation.

Development of a mathematical model and additional future studies are required to eventually determine if certain patient subgroups at risk of development of MR (ie, patients with a low coaptation reserve) may benefit from regular monitoring and appropriate timing of early intervention.

The A2-P2 was the area with the least reserve and prone to lose coaptation with annular dilation in most of the authors' patients. Although the coaptation reserve differs per patient when directly measured (raw data), it is within the expected range when the indexed value is used. It is important to realize that although the CRI is lowest at A2-P2, this does not mean that regurgitation will always occur at this location. Long-term outcomes of MR under medical treatment and after surgery are different in structural and functional diseases.[11-13] The natural history of structural regurgitation has been defined poorly due to its complex nature and because of limitations in the assessment of its severity in the past.[14] A follow-up with indexed reserve areas could be an option for a more precise follow-up.[15]

The authors' data provided additional insights into the MV coaptation zone. This study had several limitations. First, the authors' applied model was a bidimensional oversimplification of a complex structure. Second, for simplicity, they simulated a symmetrical dilation of the mitral annulus. Therefore, the prediction of imminent MR probably would be most accurate for impending Carpentier type 1 MR,[16] mitral annular dilation, pulling the leaflets away from each other. In other patients (ie, eccentric dilations of the annulus and Carpentier type II [prolapse] or III [restriction] MR), the value of repeated preregurgitation 3D TEE is more important due to the fact that the progression of MR (due to structural degenerative or functional

restrictive valvular disease) is much more difficult to predict. Third, the authors' model considered mitral leaflets as fixed structures and did not take into account leaflet remodeling[17]; this anatomic adaptation process of the MV leaflets occurs in response to stresses on the MV structure and might change coaptation reserve over time.[18,19] Fourth, coaptation reserve studies are limited in that no study can account for the stretchability of the leaflets. Finally, although the analyzed data came from 3D-data sets, the authors extracted the perfect orthogonal 2D images and/or data on which the analyses were done. The reason the authors did this was partly because they were limited by their software package and because they wanted to use easily obtainable parameters rather than 3D MV area, which is more difficult to obtain. Performing new 3D data rendering and analysis would mean writing and validating new software, which would be time-consuming and not available to everyone. The study authors used the TomTec software because it is (1) vendor-independent and (2) commercially available. The authors' calculations can be repeated by anyone (supplemental file).

In conclusion, quantification and indexing of mitral coaptation reserve along the closure line are feasible using 2D datasets derived from 3D echocardiographic data. Indexing and mathematical simulation of progressive annular dilatation, which was specific to the authors' model, consistently can be used to reveal the hypothetical area of least coaptation. This study provided a mathematical model using an individualized MV CRI for quantifying the area of contact between the anterior and posterior mitral leaflets. Additional studies are required to determine the potential "clinical" value of this mathematical model.

Conflict of Interest

Supplementary materials

Supplementary material associated with this article can be found in the online version at doi:10.1053/j.jvca.2022.11.009.

References

1 Gogoladze G, Dellis SL, Donnino R, et al. Analysis of the mitral coaptation zone in normal and functional regurgitant valves. Ann Thorac Surg 2010;89:1158–61.

2 Cobey FC, Swaminathan M, Phillips-Bute B, et al. Quantitative assessment of mitral valve coaptation using three-dimensional transesophageal echocardiography. Ann Thorac Surg 2014;97:1998–2004.

3 Nishimura RA, Otto CM, Bonow RO, et al. 2017 AHA/ACC focused update of the 2014 AHA/ACC guideline for the management of patients with valvular heart disease: A report of the American College of

Cardiology/American Heart Association Task Force on clinical practice guidelines. Circulation 2017;135:e1159–95.

4 Jeganathan J, Knio Z, Amador Y, et al. Artificial intelligence in mitral valve analysis. Ann Card Anaesth 2017;20:129–34.

5 Lancellotti P, Tribouilloy C, Hagendorff A, et al. European Association of Echocardiography recommendations for the assessment of valvular regurgitation. Part 1: Aortic and pulmonary regurgitation (native valve disease). Eur J Echocardiogr 2010;11:223–44.

6 Del Forno B, Castiglioni A, Sala A, et al. Mitral valve annuloplasty. Multimed Man Cardiothorac Surg. 2017 Oct 6;2017.

7 Sasaki H, Mahara K, Terada M, et al. Short coaptation length is a predictor of recurrent mitral regurgitation after mitral valve plasty. Heart Lung Circ 2021;30:1414–21.

8 Apostolidou E, Maslow AD, Poppas A. Primary mitral valve regurgitation: Update and review. Glob Cardiol Sci Pract 2017;2017: e201703.

9 Sorajja P, Mack M, Vemulapalli S, et al. Initial experience with commercial transcatheter mitral valve repair in the United States. J Am Coll Cardiol 2016;67:1129–40.

10 Glower D, Ailawadi G, Argenziano M, et al. EVEREST II randomized clinical trial: Predictors of mitral valve replacement in de novo surgery or after the MitraClip procedure. J Thorac Cardiovasc Surg 2012;143:S60–3.

11 Liu XM, Wu H, Zhang WK, et al. Long-term results of surgical treatment of aortic and mitral regurgitation with enlarged left ventricle. Int J Clin Exp Med 2014;7:709–13.

12 Lancellotti P, Gerard PL, Pierard LA. Long-term outcome of patients with heart failure and dynamic functional mitral regurgitation. Eur Heart J 2005;26:1528–32.

13 Antoine C, Benfari G, Michelena HI, et al. Clinical outcome of degenerative mitral regurgitation. Circulation 2018;138:1317–26.

14 Enriquez-Sarano M, Akins CW, Vahanian A. Mitral regurgitation. Lancet 2009;373:1382–94.

15 Shim H, Harloff M, Percy E, et al. Prediction for residual regurgitation after MitraClip for functional mitral regurgitation using leaflet coaptation index. J Card Surg 2020;35:3555–9.

16 Carpentier A. Cardiac valve surgery−the "French correction". J Thorac Cardiovasc Surg 1983;86:323–37.

17 Kagiyama N, Mondillo S, Yoshida K, et al. Subtypes of atrial functional mitral regurgitation: Imaging insights into their mechanisms and therapeutic implications. JACC Cardiovasc Imaging 2020;13:820–35.

18 Deferm S, Bertrand PB, Verbrugge FH, et al. Atrial functional mitral regurgitation: JACC review topic of the week. J Am Coll Cardiol 2019;73:2465–76.

19 Deferm S, Bertrand PB, Verhaert D, et al. Mitral Annular Dynamics in AF versus sinus rhythm: Novel insights into the mechanism of AFMR. JACC Cardiovasc Imaging 2022;15:1–13.